

Serial Whole-Brain Magnetization Transfer Imaging in Patients with Relapsing-Remitting Multiple Sclerosis at Baseline and during Treatment with Interferon beta-1b

Nancy D. Richert, John L. Ostuni, Craig N. Bash, Jeff H. Duyn, Henry F. McFarland, and Joseph A. Frank

BACKGROUND AND PURPOSE: To determine whether occult disease fluctuates with macroscopic lesions during the natural history of multiple sclerosis (MS) and whether therapeutic interventions affect occult disease, we performed serial monthly magnetization transfer (MT) imaging in patients with relapsing-remitting MS in a crossover trial with interferon beta-1b.

METHODS: Serial whole-brain magnetization transfer ratios (MTRs) in eight patients with relapsing-remitting MS and in four control subjects were plotted as normalized histograms, and MTR parameters were compared with contrast-enhancing lesions and bulk white matter lesion load.

RESULTS: In patients with relapsing-remitting MS, the histogram peak of 0.25 ± 0.01 and the histogram mean of 0.21 ± 0.01 were statistically lower than corresponding values in control subjects, in whom the histogram peak was 0.27 ± 0.01 and the histogram mean was 0.23 ± 0.01 . When histograms (with MTRs ranging from 0.0 to 0.5) were analyzed by quartiles (quartile 1 to quartile 4) based on histogram area, voxels with low MTRs in quartile 1 (0 to 0.12) increased during the baseline period and corresponded to bulk white matter lesion load. Interferon beta-1b reduced enhancing lesions by 91% and mean bulk white matter lesion load by 15%, but had no effect on MTR in this patient cohort.

CONCLUSION: Occult disease in normal-appearing white matter of patients with relapsing-remitting MS measured by MTR parallels the waxing and waning pattern of enhancing lesions and bulk white matter lesion load during the baseline period. MTR is not altered by interferon beta-1b, which raises the possibility of ongoing disease in normal-appearing white matter (not detected by conventional MR sequences).

MR imaging is the most sensitive and specific method of imaging disease activity and of estimating total disease burden in patients with multiple sclerosis (MS). For this reason, it has been used as a primary or secondary outcome measure in new treatment trials

of therapeutic agents (1). In most treatment trials, however, only conventional MR sequences (T1 and T2-weighted imaging) with and without contrast material have been used (2-4).

A relatively new method of estimating global disease activity in MS patients is magnetization transfer (MT) imaging. MT imaging is based on the principle that mobile (free) protons in tissues and macromolecular (bound) protons are in equilibrium (5). Selective saturation of the bound protons with an off-resonance radio frequency pulse reduces the signal intensity of the images as a result of MT. The reduction in signal intensity is expressed as the magnetization transfer ratio (MTR). Factors that affect MTR include edema and inflammation, which cause a mild reduction (5% to 8%) in MTR (6, 7) while demyelination (7-10) and axonal loss (11, 12), which disrupt the structural integrity of tissues and the macromolecular proton pool, cause a more profound reduction in MTR.

Received February 9, 1998; accepted after revision May 22.

Presented in part at the annual meeting of the International Society for Magnetic Resonance Imaging in Medicine, Vancouver, BC, April 1997.

From the Laboratory of Diagnostic Radiology Research, Clinical Center (N.D.R., J.L.O., C.N.B., J.H.D., J.A.F.) and the Neuroimmunology Branch (H.F.M.), National Institute of Neurological Diseases and Stroke, National Institutes of Health, Bethesda, MD; and the Department of Diagnostic Imaging and Radiology, Children's National Medical Center, Washington, DC (N.D.R.).

Address reprint requests to Joseph A. Frank, MD, Laboratory of Diagnostic Radiology Research, Clinical Center, National Institutes of Health, Bldg 10, Room B1N256, 10 Center Dr, Bethesda, MD 20892.

TABLE 1: Demographics and magnetization transfer ratio (MTR) histographic data in control subjects and in patients with relapsing-remitting multiple sclerosis (MS)

| Subjects | Age, y/Sex | Disease Duration, y | EDSS Score | No. of Enhancing Lesions | Bulk White Matter Lesion Load, cm ³ | MTR Peak | MTR Mean |
|-------------------------------|------------|---------------------|------------|--------------------------|--|---------------|--------------|
| Control group | | | | | | | |
| A | 50/M | | | | | 0.28 | 0.23 |
| B | 34/F | | | | | 0.28 | 0.23 |
| C | 29/M | | | | | 0.27 | 0.23 |
| D | 36/F | | | | | 0.27 | 0.22 |
| Mean (SD) | 37.2 | | | | | 0.27 (0.01) | 0.23 (0.01) |
| MS group, baseline | | | | | | | |
| 1 | 33/F | 0.5 | 1.5 | 4.0 | 1.20 | 0.25 | 0.21 |
| 2 | 26/M | 1 | 4.5 | 37.0 | 6.47 | 0.24 | 0.22 |
| 3 | 43/F | 1 | 1.0 | 3.0 | 4.87 | 0.24 | 0.21 |
| 4 | 42/F | 6 | 4.5 | 12.0 | 9.47 | 0.24 | 0.21 |
| 5 | 50/F | 3 | 2.5 | 2.4 | 5.98 | 0.23 | 0.19 |
| 6 | 39/M | 8 | 6.0 | 3.9 | 1.18 | 0.25 | 0.22 |
| 7 | 35/M | 6 | 2.0 | 1.3 | 6.91 | 0.25 | 0.21 |
| 8 | 27/M | 1 | 5.0 | 12.9 | 1.19 | 0.27 | 0.23 |
| Mean (SD) | 37 | 3.3 | 3.4 | 9.56 | 4.66 | 0.25 (0.01)** | 0.21 (0.01)* |
| MS group + interferon beta-1b | | | | | | | |
| 1 | | | 1.5 | 0.1 | 0.79 | 0.23 | 0.20 |
| 2 | | | 4.5 | 1.5 | 6.08 | 0.24 | 0.22 |
| 3 | | | 1.0 | 1.3 | 4.27 | 0.24 | 0.21 |
| 4 | | | 3.5 | 0.0 | 9.80 | 0.25 | 0.22 |
| 5 | | | 2.5 | 0.0 | 4.02 | 0.24 | 0.20 |
| 6 | | | 6.0 | 1.0 | 0.89 | 0.26 | 0.22 |
| 7 | | | 1.5 | 1.0 | 4.64 | 0.25 | 0.22 |
| 8 | | | 7.0 | 1.5 | 1.21 | 0.27 | 0.23 |
| Total (SD) | | | 3.4 | 0.81* | 3.96* | 0.25 (0.01) | 0.21 (0.01) |

Note.—*P* values for MTR were determined by the Mann Whitney test, *P* values for baseline vs. treatment by the Wilcoxin signed rank test. For both, **P* < .05 and ***P* < .01. EDSS indicates Expanded Disability Status Scale.

Dousset et al (6) first reported a wide range of MTR values in MS plaques, which they attributed to the pathologic heterogeneity of the lesions (ie, the extent of edema, demyelination, remyelination, gliosis, and axonal loss). Abnormal MTR values have also been reported in the normal-appearing white matter in MS patients (13, 14), confirming previous reports of microscopic disease based on pathologic specimens (15) and abnormal T1 relaxation times on MR imaging examinations (16). To quantitate global disease burden in MS patients, van Buchem et al (17, 18) calculated whole-brain MTR on a voxel-by-voxel basis and plotted the MTR values as a histogram. Their results showed that the height of the histographic peak was reduced in MS patients as compared with healthy control subjects, owing to a shift of voxels to lower MTR values.

To date, no serial monthly studies have been performed in MS patients to compare whole-brain MTR histograms with the natural history of the disease. The purpose of our study was to obtain longitudinal whole-brain MTR data in patients with relapsing-remitting MS and to determine whether we would observe a measurable treatment effect on MTR with interferon beta-1b.

Methods

Patient Population

Eight patients with relapsing-remitting MS were selected from a larger cohort of patients who participated in the NIH baseline-versus-treatment trial measuring the effect of interferon beta-1b on the frequency of enhancing lesions (19). The remaining patients in this large cohort were excluded because of insufficient baseline or treatment examinations to which the MT pulse sequence used in this study was applied. The demographic characteristics of the eight patients and the four healthy age-matched control subjects are summarized in Table 1. Treatment dose of interferon beta-1b was 8 mU injected subcutaneously every other day. The patients received monthly neurologic examinations, and clinical disease was evaluated by means of the Kurtzke (20) Expanded Disability Status Scale (EDSS). The study parameters were reviewed and approved by the Institutional Review Board of the National Institutes of Neurological Disease and Stroke (NINDS) at the National Institutes of Health, and informed consent was obtained for each patient.

MR Imaging

MR examinations were performed on a 1.5-T system with a standard quadrature head coil. Axial oblique interleaved sections (5-mm thick × 27 sections) were obtained with a field of view of 24 cm and a matrix of 192 × 256. MT imaging was performed before contrast administration using a T1-weighted spin-echo (SE) pulse sequence (600/16 [TR/TE]) with (M_s) and

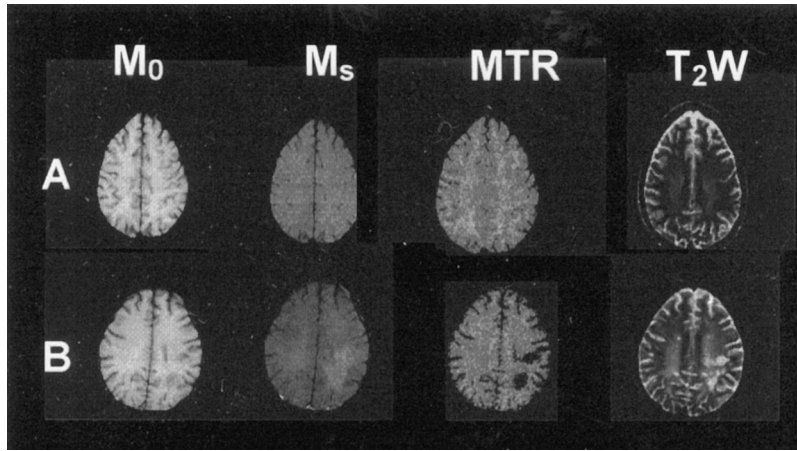


FIG 1. Representative sections from MTR analysis of a control subject (A) and a patient with relapsing-remitting MS (B). The MTR image is derived on a voxel-by-voxel basis from duplicate MT images (SE 600/16/1) obtained with (M_s) and without (M_0) a saturation pulse (1.2 kHz below water frequency) using the equation $M_0 - M_s/M_0$. T2-weighted SE images were obtained with parameters of 2000/20,100/2. Lesions in the MS patient (B), which are hyperintense on the T2-weighted image (T2W) and on the M_s image have low MTR values, approximating that of CSF.

without (M_0) a saturation pulse (16 milliseconds single lobe, 1.2 kHz below water frequency, 95° flip angle, B_1 intensity = 3.67×10^{-6} T, and three interleaved acquisitions). Dual-echo, proton density-weighted, and T2-weighted images were obtained with an SE (2000/20,100) sequence. Contrast-enhanced images were acquired 15 minutes after injection of 0.1 mmol/kg gadopentetate dimeglumine with a T1-weighted SE pulse (600/16).

Monthly MR studies were obtained in the eight patients with MS. Healthy control subjects were imaged a total of 11 times throughout the study. For all MR examinations, the specific absorption rate was below that specified in the US Food and Drug Administration guidelines.

Image Processing

Image processing was performed on a UNIX-based workstation using the medical imaging program MEDx. For each patient, the initial MT images (ie, M_0 images obtained without the saturation pulse), from the first baseline examination, served as the mapfile to which all subsequent MT images (both M_0 and M_s images) were coregistered. The image registration program, Correspondence of Closest Gradient Voxels, has been described previously (21). The mapfile also served as a “mask” image series (after manually outlining and removing the skull and extracranial tissues from each section) that was superimposed on subsequent registered MT images to define the area in which the MTR was to be computed on a section-by-section basis. MTR values were calculated on a voxel-by-voxel basis using the equation

$$MTR = (M_0 - M_s) / M_0$$

For qualitative review, color-coded images were generated in which voxel MTR was represented by increasing color intensity. A representative MT image (gray scale) is shown in Fig 1. These MT images were used for region-of-interest (ROI) MTR measurements in selected areas (25 to 50 mm³). The mean MTR values, range, standard deviation (SD), and total area of the ROI were computed using the MEDx imaging program.

The voxels were subsequently sorted into 1% bins, the number of voxels in each bin were normalized to the total number of brain voxels, and MTR values from 0.0 to 0.5 were plotted as a histogram (Fig 2A). The area under each histogram was divided into quartiles (quartile 1 to quartile 4), as shown in Figure 2A, which correspond to the 25th, 50th, 75th, and 100th percentile of the total histogram area. Quartile ranges were as follows: quartile 1 (MTR 0.0 to 0.125), quartile 2 (MTR 0.126 to 0.25); quartile 3 (MTR 0.26 to 0.37), and quartile 4 (MTR 0.38 to 0.50).

Bulk white matter lesion load was determined by a semiautomated thresholding technique that used both proton density-

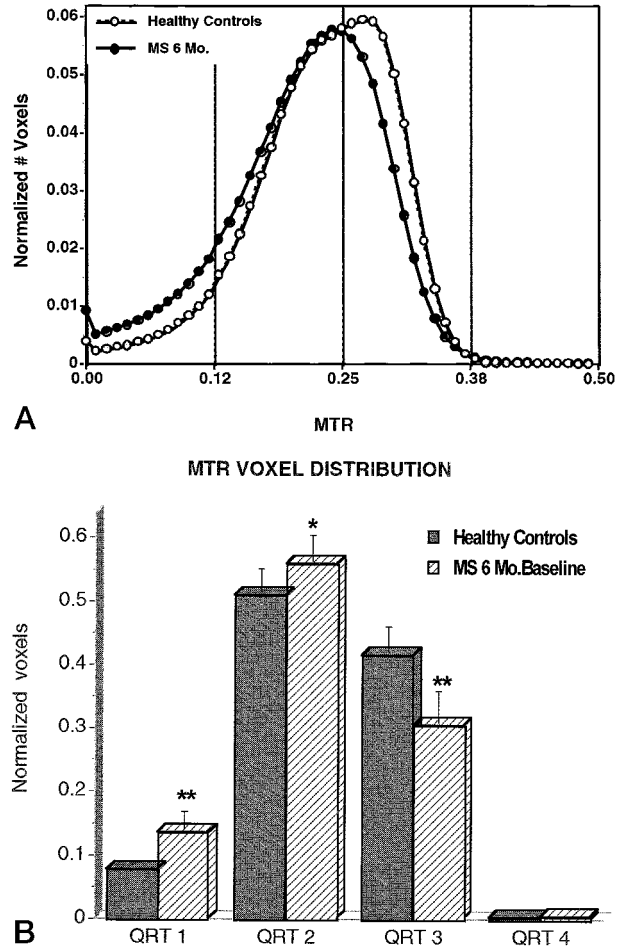


FIG 2. A, Normalized composite histogram derived from the eight patients with relapsing-remitting MS during 6 months of serial baseline examinations (closed circles) shows that the histogram peak in the MS patients is lower than that in the healthy control subjects (open circles). Histogramic areas were computed and divided into quartiles (see Methods section) with MTR ranges as follows: quartile 1 (MTR 0.0 to 0.125), quartile 2 (MTR 0.126 to 0.25), quartile 3 (MTR 0.26 to 0.37), and quartile 4 (MTR 0.38 to 0.50).

B, Bar graph representing quartile area shows the loss of voxels in quartile 3 and accumulation of voxels in quartiles 1 and 2 in patients with relapsing-remitting MS during the baseline period. Error bars represent SD. Statistical differences (two-tailed Student's *t*-test) are $P = .10$ and $^*P = .007$.

TABLE 2: Magnetization transfer ratios (MTR) determined by region-of-interest measurements in control subjects and in patients with relapsing-remitting multiple sclerosis (MS)

| Location | Control Subjects | | MS Patients | |
|-------------------------------|------------------|-----------|----------------|------------|
| | MTR | Range | MTR | Range |
| Normal-appearing white matter | 0.30 (0.02) | 0.22–0.39 | 0.27 (0.02)*** | 0.14–0.31 |
| Corpus callosum | 0.32 (0.01) | 0.26–0.39 | 0.28 (0.02)** | 0.21–0.31 |
| MS lesions | ... | ... | 0.16 (0.03)*** | 0.008–0.29 |
| Cortical gray matter | 0.21 (0.02) | 0.14–0.29 | 0.20 (0.01)* | 0.16–0.24 |
| Deep gray matter | 0.23 (0.02) | 0.17–0.32 | 0.22 (0.01) | 0.19–0.27 |

Note.—MTR values were determined by ROI measurements ($n = 15$) for control subjects with patients as described in the Methods section. The mean MTR value of all ROIs (\pm SD) is reported along with the range of MTR values in each region. P values by two-tailed Student's t -test; *** $P < .001$, ** $P < .05$, * $P < .10$.

and T2-weighted imaging (22). The total number of contrast-enhancing lesions per month were recorded from the original hard copy of each study by a consensus of two observers experienced in MR imaging of MS patients.

Statistical Analysis

Data are expressed as the mean \pm SD. Statistical significance was determined by using the following nonparametric tests: the Spearman rank correlation coefficient (SRCC) was used to compare MR imaging and clinical data (EDSS score, age, disease duration); the Mann-Whitney rank sum test was used to compare histographic MTR peak and mean data of control subjects versus patients with relapsing-remitting MS; the Wilcoxon signed rank test was used to compare baseline versus treatment with interferon beta-1b data; and Student's t -test was used for MTR ROI measurements and quartile distribution of voxels. All P values were based on a two-sided test with $P \leq .05$ considered statistically significant and $P = .10$ indicative of a trend (23).

Results

Table 1 summarizes the demographic features, clinical data, and MTR histographic data for the four healthy control subjects and the eight patients with relapsing-remitting MS during the 6-month baseline period and the 6-month period of treatment with interferon beta-1b. Figure 1 shows representative MT images from a healthy control subject (panel A) and a patient with MS (panel B), derived from the MT images obtained with (M_s) and without (M_0) the saturation pulse using the equation shown in the Methods section. The hyperintense lesions on the T2-weighted images in the MS patient also appear hyperintense on the MT image obtained with the saturation pulse (M_s) and have a low MTR, comparable to CSF, on the MT image.

To define the MTR values of gray matter and white matter, ROI measurements were made using the MT images from three control subjects and three MS patients (cases 2, 4, and 5), as shown in Table 2. Normal-appearing white matter in the MS patients had a mean MTR of 0.27 ± 0.02 , which was statistically lower than white matter in control subjects (MTR = 0.30 ± 0.01 ; $P < .001$). Callosal white matter in MS patients also had a reduced MTR (MTR = 0.28 ± 0.02) relative to that in control subjects (MTR = 0.32 ± 0.01 ; $P = .02$). The MTR of MS lesions (MTR = 0.16 ± 0.03 ; range, 0.008 to 0.29)

was significantly lower than the MTR of normal-appearing white matter ($P < .001$). Gray matter MTR in MS patients was not statistically different from that in control subjects, although there was a trend ($P = .10$) toward lower MTR in cortical gray matter in the patients with MS. The mean MTR of CSF in the lateral ventricles was 0.02 ± 0.04 .

Serial Baseline Studies

The composite MTR histogram from the eight patients with relapsing-remitting MS during the baseline period was shifted to the left of the histogram from the control subjects. The histographic peak heights were similar owing to the normalization process (Fig 2A). However, the histographic peak position in the patients with MS at MTR = 0.25 ± 0.01 was significantly lower than that in healthy control subjects at MTR = 0.27 ± 0.01 ($P = .008$). The MTR histographic mean in the patients with MS (0.20 ± 0.01) was also statistically lower than that in control subjects (0.023 ± 0.01 ; $P = .016$). These results are summarized in Table 1.

To quantitate differences in histographic parameters between the group of patients with relapsing-remitting MS and the control group, the histogram was divided into quartiles, as described in the Methods section and shown in Figure 2A. An analysis of quartile areas (Fig 2B) revealed that in the patients with MS there was an abnormal accumulation of voxels with low MTR in quartiles 1 and 2 and a corresponding loss of voxels in quartile 3. Voxels in quartile 3 represented normal-appearing white matter in MS patients and normal white matter in control subjects by ROI sampling (Table 2). The inverse correlation between voxels in quartiles 3 and 1 ($r = -.804$) and quartile 2 ($r = -.884$) was determined by linear regression analysis (data not shown). Voxels in quartile 4 represented less than 0.1% of the total brain area, and no statistical difference between patients with MS and control subjects was demonstrated ($P = .34$).

In control subjects, MTR histographic peak values were tightly clustered between 0.27 and 0.28 on all serial examinations. In contrast, there was significant interpatient variability among the patients with relapsing-remitting MS during the baseline period, with

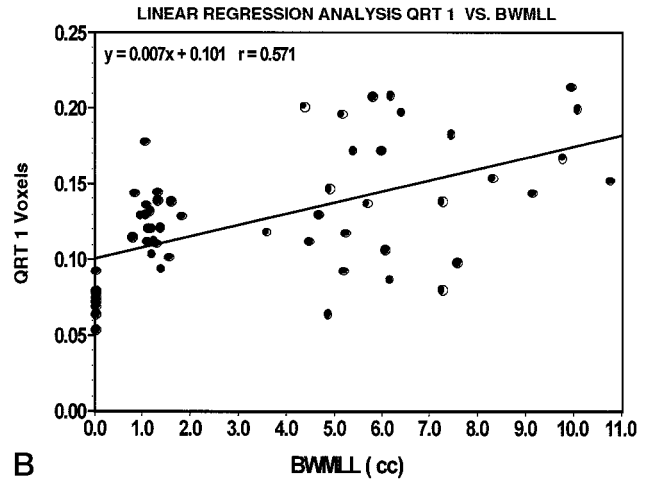
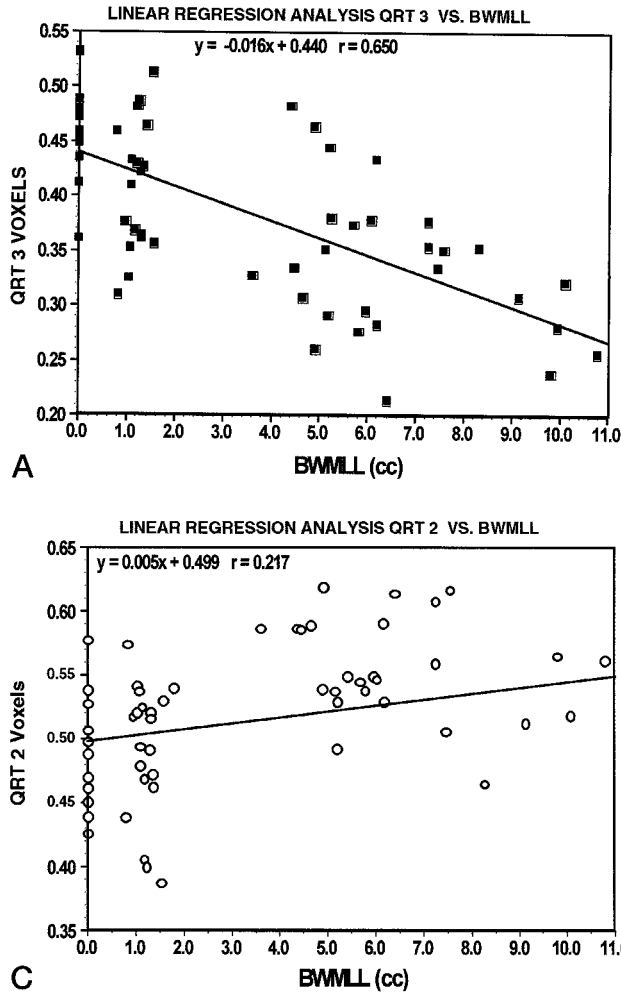


FIG 3. A, Accumulation of T2-weighted (SE 2000/20,100/2) lesions (bulk white matter lesion load [BWMLL]) in patients with relapsing-remitting MS during the baseline period corresponds to a loss of voxels in quartile (QRT) 3 ($r = .65$). B, Voxels in quartile (QRT) 1 increase with change in bulk white matter lesion load (BWMLL) in patients with MS during the baseline examinations ($r = .571$). C, Lack of correlation between voxels in quartile (QRT) 2 with accumulation of bulk white matter lesion load (BWMLL) during baseline examinations in patients with MS.

histographic peak values ranging from 0.23 to 0.27 (Table 1). No statistical correlation (SRCC) between histographic peak and patient demographic measures (eg, age, disease duration, EDSS score, or enhancing lesion frequency) was demonstrated in this small patient population. An inverse correlation between histographic peak and bulk white matter lesion load was observed but did not achieve statistical significance (SRCC = 0.619; $P = .12$). When this trend was reanalyzed by quartiles instead of by histographic peak values, a stronger correlation between bulk white matter lesion load and low MTR was observed. The results (Figure 3) show that as bulk white matter lesion load accumulates in patients with relapsing-remitting MS during the baseline period, there is a loss of voxels in quartile 3 ($r = .65$) and an increase in voxels in quartile 1 ($r = .57$), as shown in Figures 3A and B, respectively. The lack of correlation between bulk white matter lesion load and quartile 2 voxels ($r = .217$) in Figure 3C is most likely a matter of sensitivity in detecting differences, because abnormal white matter voxels in quartile 2 co-migrate with normal gray matter structures (Table 2).

The inverse correlation between bulk white matter lesion load and quartile 3 voxels is highly significant ($n = 44$; SRCC = -0.491 , $P < .001$), whereas the

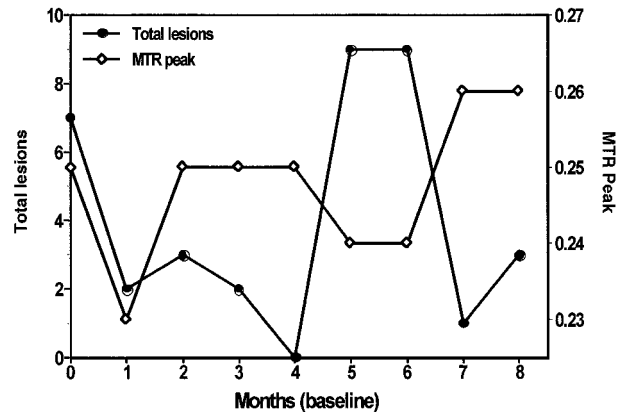


FIG 4. Sinusoidal pattern of contrast-enhancing lesions (closed circles) paralleled by inverse fluctuation in MTR histographic peak (open diamonds) in patient 6 during 8 months of baseline examinations. BWMLL, bulk white matter lesion load.

correlation between bulk white matter lesion load and quartile 1 voxels (SRCC = 0.289) is weaker ($P = .05$). These results suggest that the loss of voxels from quartile 3 and the increase of voxels in quartile 1 represent accumulating white matter disease during the baseline period.

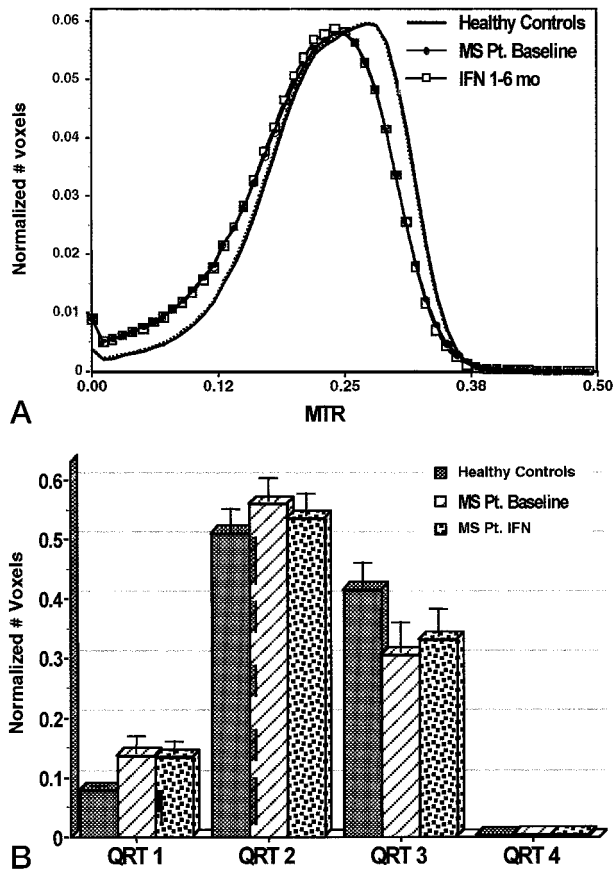


FIG 5. A, Composite normalized MTR histogram from the cohort of patients with relapsing-remitting MS during treatment with interferon (IFN) beta-1b (open squares) is unchanged from the baseline histogram (closed circles), and the histographic peak remains lower than that in control subjects (dotted line). B, Quartile (QRT) distribution during interferon beta-1b treatment (IFN) shows no redistribution of voxels.

In addition to interpatient variability there was inpatient variability in histographic peak during the baseline period, which followed the month-to-month fluctuations in the number of contrast-enhancing lesions. Figure 4 shows that during the 8-month baseline period in patient 6, the sinusoidal pattern of enhancing lesions was inversely reflected by fluctuations in histographic peak. As with enhancing lesion frequency (24), the amplitude and frequency of the change in histographic peak appeared patient-specific. No month-to-month fluctuation in histographic peak was observed in control subjects.

Effect of Interferon beta-1b Therapy

In patients with relapsing-remitting MS, interferon beta-1b caused a 91% reduction in contrast-enhancing lesions ($P = .03$) and a 15% reduction in bulk white matter lesion load ($P = .05$) but had no effect on the histographic peak or mean of the patient cohort during the first 6 months of therapy (Table 1). No additional effect of interferon beta-1b on MTR was noted when four patients were serially examined for an additional 3 to 6 months of treatment (data not

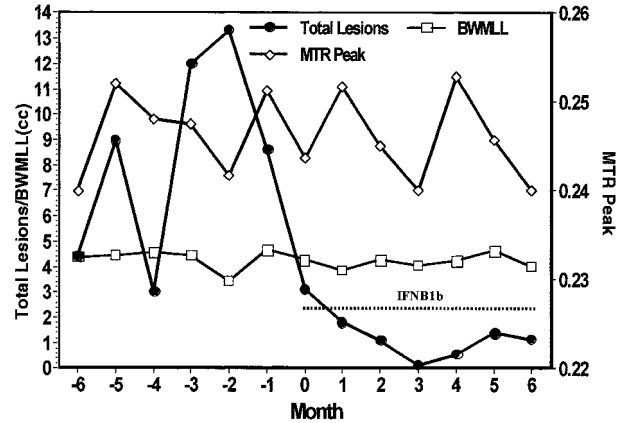


FIG 6. Serial monthly data from the MS patient cohort during baseline versus interferon beta-1b (IFNB1b) treatment show that treatment immediately reduces the mean number of contrast-enhancing lesions (closed circles) and causes a more modest reduction in bulk white matter lesion load (BWMLL) (open squares). The MTR histographic peak (open diamonds) continues to fluctuate throughout the treatment period.

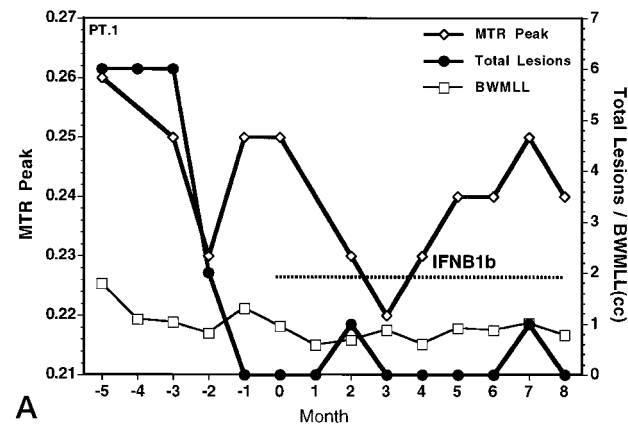
shown). There was no change in the composite histographic profile of the eight patients with MS (Fig 5A). Because the baseline studies showed a correlation between voxels in quartiles 1 and 3 and bulk white matter lesion load, we anticipated that treatment would decrease quartile 1 and increase quartile 3 in conjunction with the decrease in bulk white matter lesion load. Figure 5B shows that the quartile distribution in the patient cohort was unchanged during treatment, although linear regression analysis showed a modest decrease in quartile 1 voxels ($r = .327$) but no significant increase in quartile 3 voxels.

Analysis of the serial monthly data of the patient cohort (Fig 6) showed persistent fluctuation of the histographic peak during the treatment period despite the nearly complete suppression of enhancing-lesion activity. When individual patients were analyzed (Fig 7), the month-to-month fluctuation in histographic peak that occurred during the baseline period persisted during the treatment period despite the absence of new contrast-enhancing lesions in these patients.

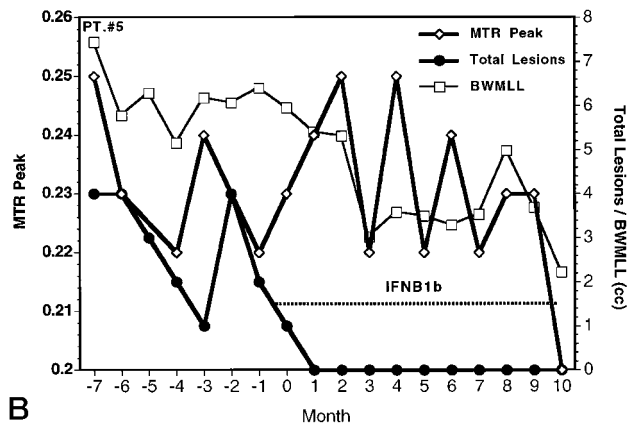
Discussion

To our knowledge, this study represents the first serial monthly MTR data in patients with relapsing-remitting MS during a drug treatment trial. MTR histographic analysis revealed that the histographic peak and mean in the patients were statistically lower than those in healthy control subjects (Fig 2A), and quartile analysis (Fig 2B) showed that this was due to voxel redistribution from quartile 3 to low MTR values in quartiles 1 and 2.

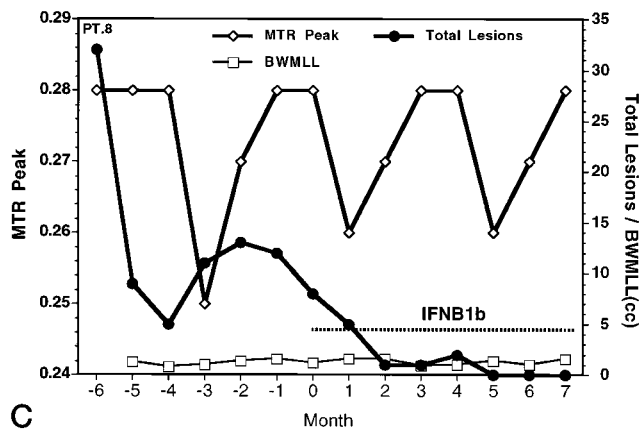
MTR values in quartile 3 correspond to voxels of normal white matter in control subjects and to normal-appearing white matter in patients with relapsing-remitting MS (Table 2). Gray matter had MTR values corresponding to quartile 2 whereas CSF (MTR = 0) was in quartile 1. In the subgroup of



A



B



C

FIG 7. A-C, Representative graphs from individual patients (cases 1, 5, and 8) show the complete suppression of contrast-enhancing lesions (*closed circles*) and reduction in bulk white matter lesion load (BWMLL) (*open squares*), but there is persistent fluctuation in MTR histographic peak (*open diamonds*). In patient 1, the mean histographic peak decreased during treatment from MTR = 0.248 to MTR = 0.236, and interferon beta-1b treatment (IFNB1b) subsequently failed in this patient. For patients 5 and 8, there is no significant change in the histographic peak.

patients examined, MS lesions were heterogeneous with MTR values, ranging from 0.11 to 0.21 (mean MTR = 0.16) confirming previous reports (6, 25–32). Thus, the majority of voxels in MS lesions would be in quartiles 1 and 2. This is supported by the correspondence between voxels in quartile 1 and bulk white matter lesion load (Fig 3B). The lack of correlation between quartile 2 and bulk white matter lesion load is most likely due to the presence of normal gray matter in quartile 2, and image segmentation may be required to detect statistically significant changes.

The results of our whole-brain histographic analysis confirm the previous findings of van Buchem et al (17, 18) that the MTR histographic peak and mean are decreased in patients with relapsing-remitting MS compared with those in healthy control subjects. However, the histographic profiles in these studies are remarkably different. In our patient cohort, the position of the histographic peak was shifted to the left of that of the control subjects. In contrast, previous investigators (17, 18) found no change in the MTR peak position but found that the MTR peak height (ie, the number of voxels in the peak) was reduced in MS patients relative to that in control subjects. The difference in the respective histograms is most likely the result of different pulse sequences and/or the offset frequency of the saturation pulse used. The patient populations also differed in that our study was composed of patients with relapsing-remitting MS with short disease duration (mean, 3.3 years)

whereas the previous study (17) included patients with a longer disease duration (mean, 9.3 years) and with more advanced, chronic progressive, MS.

The results in this study suggest that whole-brain MTR analysis provides an additional measure of white matter disease activity that tracks with contrast-enhancing lesions and bulk white matter lesion load but is not altered by interferon beta-1b treatment. Other investigators have suggested that this additional disease is microscopic and occult within normal-appearing white matter and is not detected by standard spin-echo techniques (14, 17, 18). Thus, quantitative MTR could potentially provide a more comprehensive estimate of global disease burden than do measurements of either bulk white matter lesion load or frequency of enhancing lesions.

During the baseline period, the range of MTR histographic peak values in the patients with MS correlated weakly with bulk white matter lesion load ($P = .12$). This correlation was strengthened when the voxels in individual quartiles were analyzed separately (Fig 3). Although histographic peak values fluctuated during the 12-month period of our study, no permanent change to either lower MTR (indicative of disease progression) or higher MTR (indicative of decreased lesion load, less occult disease, or possibly remyelination) was observed. This is in contrast to other reports, in which a progressive reduction of MTR occurred when patients were reexamined 20 to 30 months after their initial MTR study

(17), and suggests that a longer follow-up period may be required to observe a change.

Interferon beta-1b is thought to act at the blood-brain barrier to prevent disruptions that appear as contrast-enhancing lesions on imaging studies. The reduction of overall burden of disease (bulk white matter lesion load) in patients with relapsing-remitting MS (2, 3) is a secondary effect of interferon beta-1b that reflects the absence of new lesions and resolving inflammation in subacute lesions. At present, there is no evidence that interferons can cross an intact blood-brain barrier to block cytokine production and inflammation within chronic lesions or normal-appearing white matter (33). If MTR changes reflect only macroscopic lesion load, one would predict that interferon beta-1b would stabilize MTR or reverse the MTR histographic peak toward normal control values.

The lack of effect of interferon beta-1b on MTR could be due to the small number of patients and/or the limited period of time they were followed up during drug treatment. Alternatively, MTR may be an insensitive measure of therapeutic efficacy of this drug. The unexpected findings in this study included the fact that the mean histographic peak during interferon beta-1b treatment did not shift to higher MTR values and that the fluctuating MTR pattern was not altered by treatment despite the fact that enhancing lesions were reduced by more than 91%. It is unlikely that this oscillating pattern represents variability in pulse sequence or saturation pulse, or that it is due to artifacts in image registration, because these variations were not observed in the serial studies of healthy control subjects. These fluctuations may reflect active lesions that fail to enhance when standard conditions of contrast administration are used but that would have been detected with triple-dose (0.3 mmol/kg) contrast administration and delayed scanning techniques (34–36). Our study raises the possibility, however, that MT imaging detects changes within the normal-appearing white matter that are not affected by interferon beta-1b (eg, ongoing inflammation, edema within acute and chronic lesions, structural changes within the myelin sheath, or occult changes within normal-appearing white matter) and that are below the threshold of conventional scanning techniques (14). To pursue these possibilities, we are currently examining the MTR of individual lesions and of normal-appearing white matter using image segmentation techniques during treatment with interferon beta-1b.

With the variety of MR pulse sequences available, future MS treatment trials could be designed such that the outcome measure of MR imaging would specifically evaluate the mechanism of action of the drug being tested. For example, MTR could be used to examine therapies that suppress demyelination or promote remyelination in lesions, or therapies that stabilize oligodendrocytes from bystander damage due to cytokine or chemokine release. Alternatively, future treatment trials could be designed using a comprehensive MR evaluation protocol in which

MTR, bulk white matter lesion load, T1-weighted hypointense lesions, proton spectroscopic findings, and spinal cord atrophy are considered in an attempt to provide better correlation with clinical disability scores.

Our results suggest that MTR is a valuable tool in MS treatment trials. MTR is easily acquired with standard pulse sequences found on most MR units, and the acquisition requires only an additional 4 to 5 minutes. Image processing requires image registration to correct for minor changes in patient position between MT sequences (M_0 and M_s), which affect MTR determination. We visually check all image registrations, because incorrect registration leads to spuriously high MTR values (Richert ND, unpublished observations). Confounding technical factors in longitudinal studies of MTR include routine software and hardware upgrades on MR imaging units. Our MT saturation pulse sequence failed to perform after an upgrade, so we now use the manufacturer's MT pulse sequence and have experimentally maximized the offset frequency for a similar MT effect. In addition to controlling for drift in MTR due to software, we now scan control subjects on a monthly basis.

Given these considerations, whole-brain MTR is a sensitive measure of global disease in MS patients and reflects bulk white matter lesion load as well as microscopic occult disease. Unlike measurements of bulk white matter lesion load, the measurement of MTR is observer-independent, as no thresholding or manual tracing of lesions is required. Furthermore, the oscillating pattern of MTR suggests that this technique may be sensitive to changes in MS brain parenchyma (occult white matter disease) that have previously been undetected with conventional MR imaging sequences.

Conclusion

Compared with control subjects, patients with relapsing-remitting MS have a significantly lower whole-brain MTR, which is reflected by a shift in the histographic peak position and a decrease in the histographic mean. Serial studies demonstrate that decreases in MTR correlate with increasing disease burden, as estimated by bulk white matter lesion load. The abnormal MTR in MS patients is not measurably altered by a 6-month treatment with interferon beta-1b, despite the effective suppression of enhancing lesions and an overall decrease in bulk white matter lesion load. These results suggest that MTR provides an additional measure of disease activity or of structural changes in the myelin sheath. MTR may be a valuable tool for evaluating future therapeutic agents designed to act distal to the blood-brain barrier and to affect remyelination.

Acknowledgments

We thank the members of the Neuroimmunology Branch of NINDS who participated in this crossover trial, particularly Lael Stone, who served as the clinical fellow for this patient

cohort, and Roger Stone, who performed data management. We also acknowledge the nursing staff and MRI staff who were actively involved in this project, especially Bobbi Lewis, Jeanette Black, and Rene Hill.

MEDx image processing software is a product of Sensor Systems Inc, Reston, Va, www.sensor.com.

References

- Miller DH, Albert PS, Barkhof F, et al. **Guidelines for the use of magnetic resonance techniques in monitoring the treatment of multiple sclerosis.** *Ann Neurol* 1996;39:6-16
- Paty DW, Li DKB, UBC MS/MRI Study Group, IFNB Multiple Sclerosis Study Group. **Interferon beta 1b is effective in relapsing-remitting multiple sclerosis, II: MRI analysis result of a multicenter randomized, double-blind, placebo-controlled trial.** *Neurology* 1993;43:662-667
- Stone LA, Frank JA, Albert PS, et al. **The effect of interferon-beta on blood-brain barrier disruptions demonstrated by contrast-enhanced magnetic resonance imaging in relapsing/remitting multiple sclerosis.** *Ann Neurol* 1995;37:611-619
- Jacobs LD, Cookfair DI, Rudick RA, et al. **Intramuscular interferon beta-1a for disease progression in relapsing multiple sclerosis.** *Ann Neurol* 1996;39:285-294
- Wolff SD, Balaban RS. **Magnetization transfer contrast (MTC) and tissue water proton relaxation in vivo.** *Magn Reson Med* 1989;10:135-144
- Dousset V, Grossman RI, Ramer KN, et al. **Experimental allergic encephalomyelitis and multiple sclerosis: lesion characterization with magnetization transfer imaging.** *Radiology* 1992;182:483-491
- Mehta RC, Pike GB, Enzmann D. **Measure of magnetization transfer in multiple sclerosis demyelinating plaques, white matter ischemic lesions, and edema.** *AJNR Am J Neuroradiol* 1996;17:1051-1055
- Dousset V, Brochet B, Vital A, et al. **Lysolecithin-induced demyelination in primates: preliminary in vivo study with MR and magnetization transfer.** *AJNR Am J Neuroradiol* 1995;16:225-231
- Kasner SE, Galetta SL, McGowan JC, et al. **Magnetization transfer imaging in progressive multifocal leukoencephalopathy.** *Neurology* 1997;48:534-536
- Dousset V, Armand JP, Lacoste D, et al. **Magnetization transfer study of HIV encephalitis and progressive multifocal leukoencephalopathy.** *AJNR Am J Neuroradiol* 1997;18:895-901
- Lexa FJ, Grossman RI, Rosenquist AC. **MR of wallerian degeneration in the feline visual system: characterization by magnetization transfer rate with histopathologic correlation.** *AJNR Am J Neuroradiol* 1994;15:201-212
- Kimura H, Meaney DF, McGowan JC, et al. **Magnetization transfer imaging of diffuse axonal injury following experimental brain injury in the pig: characterization by magnetization transfer ratio with histopathologic correlation.** *J Comput Assist Tomogr* 1996;20:540-546
- Filippi M, Campi MD, Dousset V, et al. **A magnetization transfer imaging study of normal-appearing white matter in multiple sclerosis.** *Neurology* 1995;45:478-482
- Loevner LA, Grossman RI, Cohen JA, Lexa FJ, Kessler D, Kolso DL. **Microscopic disease in normal-appearing white matter on conventional MR images in patients with multiple sclerosis: assessment with magnetization-transfer measurements.** *Radiology* 1995;196:511-515
- Allen IV, McKeown SR. **A histological, histochemical and biochemical study of the macroscopically normal white matter in multiple sclerosis.** *J Neurol Sci* 1979;41:81-91
- Barbosa S, Blumhardt LD, Roberts N, Lock T, Edwards RHT. **Magnetic resonance relaxation time mapping in multiple sclerosis: normal appearing white matter and the "invisible" lesion load.** *J Magn Reson Imaging* 1994;12:33-42
- van Buchem MA, McGowan JC, Kolson DL, Polansky M, Grossman RI. **Quantitative volumetric magnetization transfer analysis in multiple sclerosis: estimation of macroscopic and microscopic disease burden.** *Magn Reson Med* 1996;36:632-636
- van Buchem MA, Udupa JK, McGowan JC, et al. **Global volumetric estimation of disease burden in multiple sclerosis based on magnetization transfer imaging.** *AJNR Am J Neuroradiol* 1997;18:1287-1290
- Stone LA, Frank JA, Albert PS, et al. **Characterization of MRI response to treatment with interferon beta-1b: contrast-enhancing MRI lesion frequency as a primary outcome measure.** *Neurology* 1997;49:862-869
- Kurtzke JF. **Rating neurologic impairment in multiple sclerosis: an expanded disability status scale (EDSS).** *Neurology* 1983;33:1444-1452
- Ostuni JL, Levin RL, Frank JA, DeCarli C. **Correspondence of closest gradient voxels: a robust registration algorithm.** *J Magn Reson Imaging* 1997;7:410-415
- DeCarli C, Maisog J, Murphy DGM, Teichberg D, Rapoport SI, Horwitz B. **Method for quantification of brain, ventricular and subarachnoid CSF volumes from MR images.** *J Comput Assist Tomogr* 1992;16:274-284
- Glantz SA. *Primer of Biostatistics.* 4th ed. New York: McGraw Hill; 1997;8:213-281
- Stone LA, Frank JA, Albert PS, et al. **Characterization of MRI response to treatment with interferon beta-1b: contrast-enhancing MRI lesion frequency as a primary outcome measure.** *Neurology* 1997;49:862-869
- Gass A, Barker GJ, Kidd D, et al. **Correlation of magnetization transfer ratio with clinical disability in multiple sclerosis.** *Ann Neurol* 1994;36:62-67
- Tomiak MM, Rosenblum JD, Prager JM, Metz CE. **Magnetization transfer: a potential method to determine the age of multiple sclerosis lesions.** *AJNR Am J Neuroradiol* 1994;15:1569-1574
- Lai HM, Davie CA, Gass A, et al. **Serial magnetization transfer ratios in gadolinium-enhancing lesions in multiple sclerosis.** *J Neurol* 1997;244:308-311
- Hiehle JF, Grossman RI, Ramer KN, Gonzalez-Scarano F, Cohen JA. **Magnetization transfer effects in MR-detected multiple sclerosis lesions: comparison with gadolinium-enhanced spin-echo images and nonenhanced T1-weighted images.** *AJNR Am J Neuroradiol* 1995;16:69-77
- Petrella JR, Grossman RI, McGowan JC, Campbell G, Cohen JA. **Multiple sclerosis lesions: relationship between MR enhancement pattern and magnetization transfer effect.** *AJNR Am J Neuroradiol* 1996;17:1041-1049
- Loevner LA, Grossman RI, McGowan JC, Ramer KN, Cohen JA. **Characterization of multiple sclerosis plaques with T1-weighted MR and quantitative magnetization transfer.** *AJNR Am J Neuroradiol* 1995;1473-1479
- Hiehle JF, Lenkinski RE, Grossman RI, et al. **Correlation of spectroscopy and magnetization transfer imaging in the evaluation of demyelinating lesions and normal appearing white matter in multiple sclerosis.** *Magn Reson Med* 1994;32:285-293
- Kimura H, Grossman RI, Lenkinski RE, Gonzalez-Scarano R. **Proton MR spectroscopy and magnetization transfer ratio in multiple sclerosis: correlative findings of active versus irreversible plaque disease.** *AJNR Am J Neuroradiol* 1996;17:1539-1547
- Smith RA, Norris F, Palmer D, Bernhardt L, Wills RJ. **Distribution of alpha interferon in serum and cerebrospinal fluid after systemic administration.** *Clin Pharmacol Ther* 1985;37:85-88
- Filippi M, Yousry T, Campi A, et al. **Comparison of triple dose versus standard dose gadolinium-DTPA for detection of MRI enhancing lesions in patients with MS.** *Neurology* 1996;46:379-384
- van Waesberghe JH, Castelijns JA, Roser W, et al. **Single-dose gadolinium with magnetization transfer versus triple-dose gadolinium in the MR detection of multiple sclerosis lesions.** *AJNR Am J Neuroradiol* 1997;18:1279-1285
- Silver NC, Good CD, Barker GJ, et al. **Sensitivity of contrast enhanced MRI in multiple sclerosis: effects of gadolinium dose, magnetization transfer contrast and delayed imaging.** *Brain* 1997;120:1149-1161